

Article

Flow through and Volume Change Behavior of a Compacted Expansive Soil Amended with Natural Biopolymers

Ahmed Bukhary  and Shahid Azam * 

Environmental Systems Engineering, University of Regina, 3737 Wascana Parkway, Regina, SK S4S 0A2, Canada; ahb949@uregina.ca

* Correspondence: shahid.azam@uregina.ca

Abstract: Natural biopolymers offer a sustainable alternative for improving soil behavior due to their inert nature, small dosage requirement, and applicability under ambient temperatures. This research evaluates the efficacy of natural biopolymers for ameliorating an expansive soil by using a 0.5% dosage of cationic chitosan, charge-neutral guar gum, and anionic xanthan gum during compaction. The results of laboratory investigations indicate that the flow through and volume change properties of the expansive soil were affected variably. The dual porosity, characterized by low air entry due to inter-aggregate pores (AEV_1 of 4 kPa) and high air entry due to the clay matrix (AEV_2 of 200 kPa) of the soil, was healed using chitosan and guar gum (AEV of 200 kPa) but was enhanced by the xanthan gum (AEV_1 of 100 kPa and AEV_2 of 200 kPa). The s-shaped swell–shrink path of the soil comprised structural (e from 1.23 to 1.11), normal (e from 1.11 to 0.6), and residual stages (e ranged from 0.6–0.43). This shape was converted into a j -shaped path through amendment using chitosan and guar gum, showing no structural volume change, with e from about 1.25 to 0.5, but was reverted to a more pronounced form by xanthan gum, with e from 1.5 to 1.32, 1.32 to 0.49, and 0.49 to 0.34 in the three stages, respectively. The consolidation behavior of the soil was largely unaffected by the addition of biopolymers such that the saturated hydraulic conductivity decreased from 10^{-9} m/s to 10^{-12} m/s over a void ratio decrease from 1.1 to 0.6. At a seating stress of 5 kPa, the swelling potential (7.8%) of the soil slightly decreased to 6.9% due to the addition of chitosan but increased to 9.4% and 12.2% with guar gum and xanthan gum, respectively. The use of chitosan and guar gum will allow the compaction of the investigated expansive soil on the dry side of optimum.



Citation: Bukhary, A.; Azam, S. Flow through and Volume Change Behavior of a Compacted Expansive Soil Amended with Natural Biopolymers. *Geotechnics* **2024**, *4*, 322–336. <https://doi.org/10.3390/geotechnics4010017>

Academic Editor: Abbas Taheri

Received: 13 February 2024

Revised: 16 March 2024

Accepted: 19 March 2024

Published: 20 March 2024



Copyright: © 2024 by the authors. Licensee MDPI, Basel, Switzerland. This article is an open access article distributed under the terms and conditions of the Creative Commons Attribution (CC BY) license (<https://creativecommons.org/licenses/by/4.0/>).

1. Introduction

Natural biopolymers (derived from plants, animals, and microorganisms) constitute a new and sustainable class of materials for ameliorating the geotechnical behavior of expansive soils [1]. These long-chained organic additives are characterized by high hydrophilicity, gelation ability, and a variable charge type and density [2–4]. As such, they can readily interact with the negative charges on the large specific surface areas of expansive clay minerals. Typically, biopolymers require small dosages of up to 2% that can be applied at ambient field temperatures [5] and are generally inert in nature [6]. The major drawback of using these admixtures is their potential biodegradation arising from exposure to wet–dry and freeze–thaw cycles, thereby causing durability issues [7]. More importantly, the lack of standardized terminology and manufacturers' reluctance to disclose proprietary product information constitute significant hurdles to developing a clear understanding of how these materials interact with active clay particles in the presence of water [8]. Given that published data are relatively scarce, there is a need to investigate the efficacy of these cost-effective, environmentally friendly, and socially acceptable materials for improving volumetric changes due to water ingress and removal in compacted expansive soils.

The most common biopolymers used for the stabilization of expansive soils are chitosan (cationic), guar gum (charge-neutral), and xanthan gum (anionic). Generally, these polysaccharides (monosaccharide units bound together by glycosidic bonds) possess molecular weights in the range of 10^4 mg/mol to 10^7 mg/mol [9]. Chitosan is derived from chitin (poly(β -[1,4]-N-acetyl-d-glucosamine)), which is present in the cell walls of fungi and the exoskeletons of insects and crustaceans [9]. This cationic biopolymer is obtained by removing the acetyl group in chitin using a concentrated alkali such as NaOH or KOH at an elevated temperature between 90 °C and 120 °C [10,11]. In contrast, guar gum is extracted from the endosperm of the cluster bean (*Cyamopsis tetragonolobus*) [12,13]. This charge-neutral biopolymer (purified endosperm) comprises a galactose group ($C_6H_{12}O_6$) attached to a central mannose group ($C_6H_{12}O_6$) [13,14]. Finally, xanthan gum is formed through the fermentation of plant-based glucose using the *Xanthomonas campestris* bacterium. This anionic biopolymer has the molecular formula of $C_{35}H_{49}O_{29}$ and comprises D-uronic acid, D-mannose, pyruvylated mannose, 6-O-acetyl D-mannose, and 1, 4-linked glucan [15,16].

Table 1 summarizes the generic properties of the three biopolymers. The three types of biopolymers cover the entire range of charges and interact with expansive soils mostly by electrostatic attractions through which the biopolymer chains are adsorbed [2]. Depending on the biopolymer charge, adsorption takes place in three different modes: (i) directly due to the positive amine group ($-NH_2$) of cationic chitosan, (ii) indirectly because of the dipolar attraction of the hydroxyl group (OH^-) of neutrally charged guar gum [3,17], and (iii) indirectly owing to the counter-ions in the solution involving the carboxyl group ($COOH-$) of anionic xanthan gum. The efficacy of these interactions depends on several factors such as the biopolymer dosage and molecular weight, the charge density and specific surface area of the clay, and the type and number of ions in the pore fluid [3,18]. Nonetheless, adsorption occurs by means of one of two primary mechanisms: bridging, in which the convoluted loops, trains, and tails of the biopolymer chains loosely attach to adjacent clay surfaces, and charge patching, where available sections of biopolymer chains attach to partially exposed sites on the clay particle surfaces [2,19]. Furthermore, a hydrogel (a system of cross-linked biopolymer chains containing a portion of the pore water) is formed that partially fills the void spaces between the newly developed particle assemblages [20,21]. These conceptual mechanisms are operative when the admixture is added to expansive clays and the soil layer is prepared for compaction. Post-compaction, the flow through and volume changes depend on the soil [1,22,23].

Table 1. Summary of generic properties of biopolymers.

Biopolymer	Charge	Appearance	Viscosity (cps)	Other
Chitosan	Cationic	Off-white to beige and faint brown to light brown powder and/or chips	200–800	Deacetylation $\geq 75\%$
Guar gum	Neutral	White to faint to yellow, beige or brown powder	-----	Loss on drying $\leq 13\%$ Total ash $\leq 1\%$
Xanthan gum	Anionic	Faint yellow to yellow to beige powder	800–1200	-----

Recent experiences with the use of biopolymers indicate an improvement in the flow through and volume change properties of compacted soils. For example, Manzanal et al. [24] reported an increase in the air entry value (AEV) from 300 kPa to 600 kPa for a high-plasticity silt from Comodoro, Argentina, when 0.5% (dry mass basis) of anionic calcium lignosulfonate was used. Likewise, the water content has been reported to increase by 5% for a loamy soil from Maragheh, Iran [25], and by 100% for a sandy clay from Jumunjin, Korea [26], for 1% cationic chitosan and 0.75–1% anionic xanthan gum, respectively. The saturated hydraulic conductivity (k_s) was observed to decrease for a poorly graded sand from Songkhla, Thailand, by almost three orders of magnitude (from 6.9×10^{-5} m/s to 2.3×10^{-8} m/s) when 22.5% of anionic para rubber was used [27]. However, k_s is also reported to increase for highly plastic clay from Hong Kong by one order of magnitude

(from 1.2×10^{-9} m/s to 1.3×10^{-8} m/s) for 20% anionic biochar [28]. In a similar way, the compression index (C_c) and the swell index (C_s) have shown changes for lean clays (Shanghai, China, and Warangal, India) by ± 0.06 and ± 0.04 when amended with 0.5–4% charge-neutral guar gum as well as anionic xanthan gum and a 1–4% mixture of anionic carrageenan and charge-neutral casein, respectively [29–31]. These improvements are material-specific and as such should be extended to the local expansive soil that severely affects the construction and maintenance of civil infrastructure in the region.

The main objective of this paper was to develop a basic geotechnical understanding of the flow through and volume change behavior of compacted expansive soils amended with natural biopolymers. Clay with known engineering properties was compacted, and three distinct biopolymers (cationic chitosan, charge-neutral guar gum, and anionic xanthan gum) were added at the optimum conditions. The water retention curve (WRC) and the swell-shrink curve (SSC) were developed to characterize the unsaturated soil properties, whereas the consolidation curve and the hydraulic conductivity were determined to understand the saturated soil behavior.

2. Research Methodology

The soil was obtained from 47 test pits in Regina, Saskatchewan, Canada. The samples were retrieved from 0.15 m to 2.0 m depths, sealed in plastic, collectively placed in 20 L plastic buckets, and transported to the Saskatchewan Advanced Geotechnical Engineering (SAGE) laboratory at the University of Regina in accordance with ASTM D4220/D4220M-14. The soil was air-dried, chunks were broken down, and coarse particles and grass roots were removed. A representative soil composition was obtained by mixing all the samples, pulverizing them using a grinder, and discarding material coarser than 4.75 mm. A comprehensive laboratory investigation program was enacted to determine the geotechnical properties of the expansive soil amended with biopolymers. Table 2 provides a summary of the test type and number of samples.

Table 2. Summary of laboratory investigation program showing number of samples used for various tests and materials.

Test Type	Un-Amended	Chitosan-Amended	Guar Gum-Amended	Xanthan Gum-Amnded
Specific Gravity	3	----	----	----
Sieve and Hydrometer	1	----	----	----
Consistency Limits	3	----	----	----
Compaction Curve	6	----	----	----
Compacted Sample *	2	2	2	2
Saturation Time	16	----	----	----
Water Retention	12	10	12	10
Swell-Shrink	12	10	12	10
Consolidation	1	1	1	1

* Used to extract sub-samples for subsequent laboratory testing.

The index properties were determined for the expansive soil using the following ASTM standard methods: (i) grain size distribution by D422-63(2007)e2 and D7928-21e1; (ii) specific gravity (G_s) by D854-14; and (iii) liquid limit (w_L), plastic limit (w_p), and plasticity index (I_p) by D4318-17e1. The shrinkage limit (w_s) was determined using the plasticity chart following the method described in [32]. The soil was classified per D2487-17e1.

The compaction curve for the expansive soil was developed according to Method A in D698-12e2. The air-dried soil was mixed with predetermined amounts of distilled water, and the mixture was sealed in double plastic bags to equilibrate over 24 h. Thereafter, the mix was placed in a steel mold (101 mm diameter and 154 mm height) and compacted in three equivalent layers using 25 blows/layer. The water content (w) was determined using D2216-19, and the dry unit weight (γ_d) was determined from the mass and volume of the compacted sample using phase relationships.

The biopolymers were provided by MilliporeSigma Canada Limited. Proprietary data on the biopolymer composition are not available. Nonetheless, the selected biopolymers cover the entire range of charges to affect the flow through and volume change behavior of the investigated expansive soil. A biopolymer dosage of 0.5% (dry mass basis) was selected to improve both the flow through and volume change in the expansive soil while developing a workable material [24,33–35]. The dry mixing method described in [15] was used, where the powdered biopolymer was gently mixed with the air-dried soil. Next, distilled water (equivalent to the optimum water content) was added; a 1% acetic acid solution was used for chitosan to ensure a thorough dissolution of this biopolymer. Lumps that formed due to the high viscosity and hydrophilicity of the biopolymers were broken down by gently pressing against them using a spatula. The biopolymer-amended soil samples were sealed in plastic bags, allowed to equilibrate over 24 h, and compacted as described before.

For use in subsequent testing, the time required to saturate the clay was determined. Two sets of identical sub-samples were obtained from the optimally compacted sample: smaller samples (35 mm diameter and 13 mm thick) for the WRC and larger samples (63 mm diameter and 20 mm thick) for consolidation. Each set of samples was confined in metal rings to prevent lateral deformation, allowed to saturate with distilled water in both single and double drainage modes, and sealed in plastic containers to minimize evaporation. One sample from each set was obtained from the containers at fixed time intervals of 6, 24, 48, and 72 h. Excess water was removed, and the sample was divided into two sub-specimens for the determination of w (as before) and void ratio (e). The latter property was determined by coating the specimen of a known mass with molten wax ($G_s = 0.90$) and submerging it in a beaker filled with distilled water to determine the volume. The sample volume (obtained from the displaced water volume) was corrected to account for the wax volume underestimation arising from possible air entrapment at the soil-wax interface [36]. The degree of saturation (S) was determined from phase relationships and plotted with respect to time.

The WRC was determined as per ASTM D6836-16 using a pressure porous plate and a porous membrane to apply suction (ψ) values of up to 400 kPa and up to 2000 kPa, respectively. Identical sub-samples (35 mm diameter and 13 mm thick) were obtained from the optimally compacted sample. Ten to twelve sub-samples were placed on corresponding plates/membranes and allowed to saturate in double drainage conditions using distilled and de-aired water. Full saturation was achieved in three days. The selected suction increments were applied and frequently monitored to ensure a consistent value. This was achieved by observing the water level in a graduated burette that was duly connected to the extractor chamber. The test was terminated when consecutive readings showed a negligible difference over 24 h; w , e , and S were determined as before. For high suction values ($\psi > 2000$ kPa), a dew point potentiometer (WP4-T) was employed. A 10 g sub-sample was cut from the compacted sample and placed in a sampling cup, which was then carefully positioned in the potentiometer chamber. The device displayed a suction reading on the output screen when the vapor pressure in the soil equilibrated with the vapor pressure in the surrounding air. The equilibration time increased with suction and generally varied from a few minutes to about one hour. Again, the water content was determined as before.

The SSC was determined using two different methods. For a high water content ($w > w_p$), the ASTM D4943-18 standard was used wherein the sub-samples retrieved from the pressure extractors were divided into two specimens, and w and e were determined as described before. For a low water content ($w < w_p$), a Vernier caliper and a sensitive balance were used to determine e . In this case, a sub-sample (35 mm diameter and 13 mm) was cored from the compacted sample and allowed to air-dry. The decrease in the mass and volume of the sub-sample was recorded at specific time intervals and used to determine w and e , respectively.

The volume change properties were investigated in two distinct steps. A sub-sample (63 mm diameter and 20 mm thick) was retrieved from the compacted sample, as mentioned

before, and inundated with water at a seating stress of 5 kPa. Initially, the swelling potential was measured following ASTM D4546-14e1 until successive data points over one week were observed to be insignificant. Thereafter, the sample was incrementally loaded under consolidation according to Method B in ASTM D2435/D2435M-11. A digital camera was set up to register the deformations using a dial gauge at defined time intervals. The entire test data were analyzed to determine the consolidation parameters (coefficient of volume compressibility (m_v) and coefficient of consolidation (c_v)) which, in turn, were used to determine the saturated hydraulic conductivity (k_s) in accordance with the method described by [37].

3. Results and Discussion

Table 3 gives the geotechnical index properties for the investigated soil such that the data were similar to previous studies on this glacio-lacustrine clay deposit [38–41]. The G_s of 2.71 indicated the possible presence of clay minerals. Likewise, the grain size distribution curve (Figure 1) shows that the amount of material finer than 0.075 mm and 0.002 mm was 90% and 65%, respectively. The measured liquid limit ($w_L = 71\%$), plastic limit ($w_P = 27\%$), and estimated shrinkage limit ($w_S = 14.5\%$) indicated a high water adsorption capacity. Overall, the investigated clay was classified as CH (highly plastic clay) as per the Unified Soil Classification System (USCS).

Table 3. Summary of geotechnical index properties of the investigated expansive soil.

Soil Property	Mean Value	Range of Values
Specific gravity, G_s	2.71	2.70–2.72
Material finer than 4.75 mm (%)	100	----
Material finer than 0.075 mm (%)	90	----
Material finer than 0.002 mm (%)	65	----
Liquid limit, w_L (%)	71	70–72
Plastic limit, w_P (%)	27	26–28
Shrinkage limit, w_S (%)	14.5	14–15
USCS symbol	CH	----

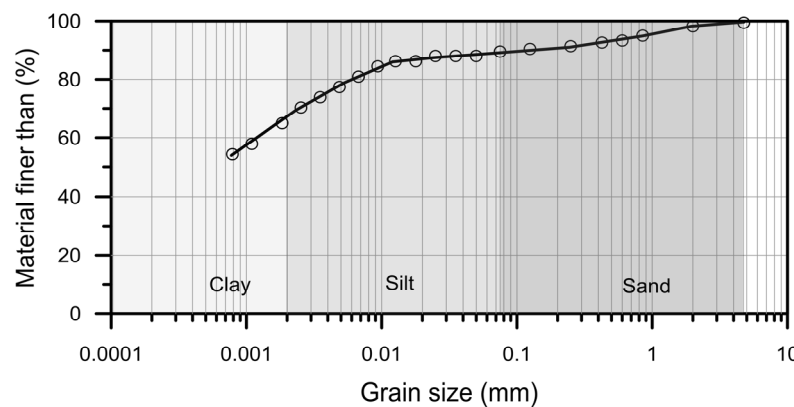


Figure 1. Grain size distribution of the investigated expansive soil.

Figure 2 gives the compaction curve for the investigated expansive clay with theoretical S lines based on $G_s = 2.71$. The maximum dry unit weight ($\gamma_{d-max} = 14.9 \text{ kN/m}^3$) and the optimum water content ($w_{opt} = 25.5\%$) were found to be similar to previous studies using the standard Proctor test: 14.2 kN/m^3 and 26% [40] and 14.8 and 28.5% [42]. As expected, γ_d increased dry of optimum due to pore air expulsion and particle re-arrangement and decreased wet of optimum due to pore water infilling and particle swelling [43,44].

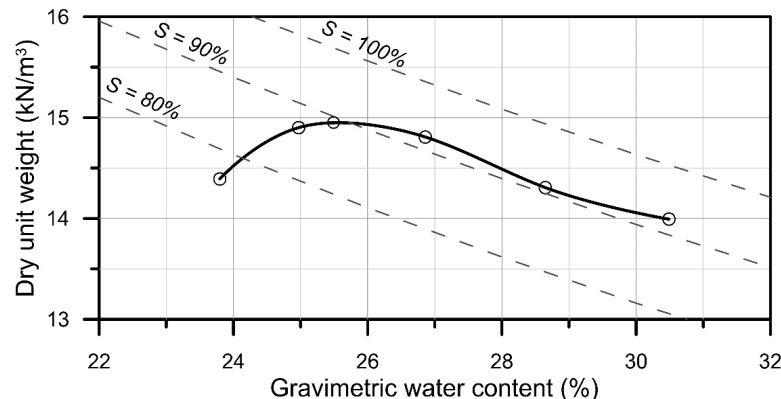


Figure 2. Compaction curve of the investigated expansive soil.

Generally, the fabric of compacted expansive soils on the dry side of optimum comprises a bimodal pore size distribution. The inter-aggregate macropores between the clay clods have a mean radius of 4 μm , and the intra-aggregate micropores within the clay clods have radii of about 0.3 μm . In contrast, the microstructure of compacted expansive soils on the wet side of optimum consists of a unimodal pore size distribution with only 0.5 μm radii intra-aggregate micropores within the clods [45–47]. Along the compaction curve, an increasing water content results in clay swelling, thereby increasing the soil compressibility under subsequent loading [40]. The immovable water films around the clay particles decrease the available flow paths for water movement and as such decrease k_s [48]. At the maximum γ_d , compressibility reaches a minimum value because further reduction in void ratio is difficult to achieve during consolidation [49]. The k_s value is also at a minimum and is attributable to the maximum tortuosity, which is the ratio of the convoluted flow paths to the straight path [50].

Figure 3 gives the change in S versus time for two sample sizes and two drainage modes for the optimally compacted ($w = 25.5\%$, $\gamma_{d-\max} = 14.9 \text{ kN/m}^3$) sample corresponding to an $S = 88.5\%$. All the samples showed an initial sharp increase due to the water migration through both the inter-aggregate and intra-aggregate pores, followed by a relative flat increase due to the water movement within the intra-aggregate pores only [44,47]. The time to saturation was found to be 72 h. The double drainage mode resulted in a relatively faster saturation because the flow path was reduced to half the sample height. For the same reason, the smaller samples (13 mm thick) saturated quicker than the larger samples (20 mm thick).

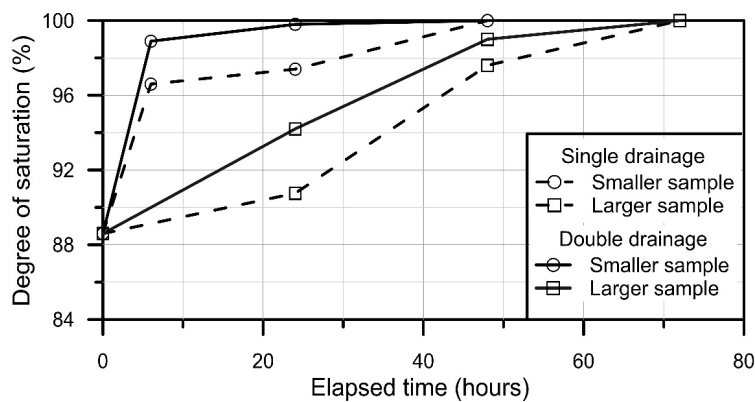


Figure 3. Saturation versus time curves for the optimally compacted expansive soil.

Figure 4 gives the w -based WRC for the investigated clay amended with biopolymers. The test data are used to develop best-fit curves based on observation and experience. The initial water content was assigned an arbitrary low suction value of 1 kPa. Similar

to previous work on local expansive clay, the unamended sample (Figure 4a) showed a bimodal path with a low AEV₁ (4 kPa) corresponding to capillary water drainage through the inter-aggregate pores and a high AEV₂ (200 kPa) attributed to the flow through the intra-aggregate pores in the soil matrix [40].

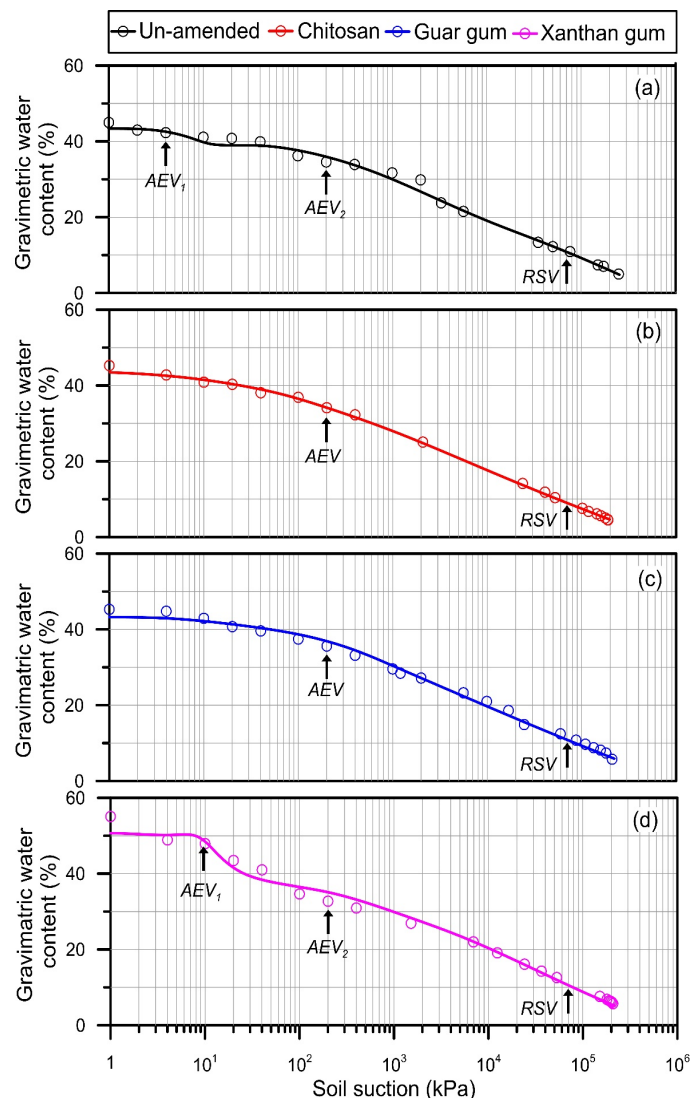


Figure 4. Water retention curves for the optimally compacted expansive soil: (a) unamended and amended with (b) chitosan; (c) guar gum; (d) xanthan gum.

The chitosan-amended soil (Figure 4b) and the guar-gum-amended soil (Figure 4c) showed unimodal paths with an AEV = 200 kPa. For these admixtures, the formation of a hydrogel resulted in developing a homogenous clay matrix with a uniform pore size distribution available for water migration [51]. The xanthan-gum-amended soil (Figure 4d) showed a bimodal path with an AEV₁ of 10 kPa and a similar AEV₂ (200 kPa). For this biopolymer, an AEV₁ of more than double the unamended soil suggests partial healing of the inter-aggregate pores due to the possible insufficiency of the cations for bridging at the applied dosage. The consistent values of matrix air entry (200 kPa) and residual suction (70×10^3 kPa) for all the samples indicate that biopolymers affect water retention primarily at low values of soil suction.

Figure 5 and Table 4 give the SSC for the investigated expansive clay, with the theoretical degree of saturation lines developed using phase relationships and $G_s = 2.71$. The test data are used to develop best-fit curves based on observation of the test results and

experience with this expansive clay. The unamended soil (Figure 5a) showed a typical *s*-shaped SSC [52]. Starting from the initially saturated state, the curve exhibited (i) *structural shrinkage* (e from 1.23 to 1.11), with a relatively flat slope due to the water removal from the inter-aggregate pores; (ii) *normal shrinkage* (e from 1.11 to 0.6), with a predominantly steep slope due to water removal from the intra-aggregate pores; and (iii) *residual shrinkage*, (e from 0.6 to 0.43) with an essentially flat slope due to water leaving the particle surface in the clay matrix.

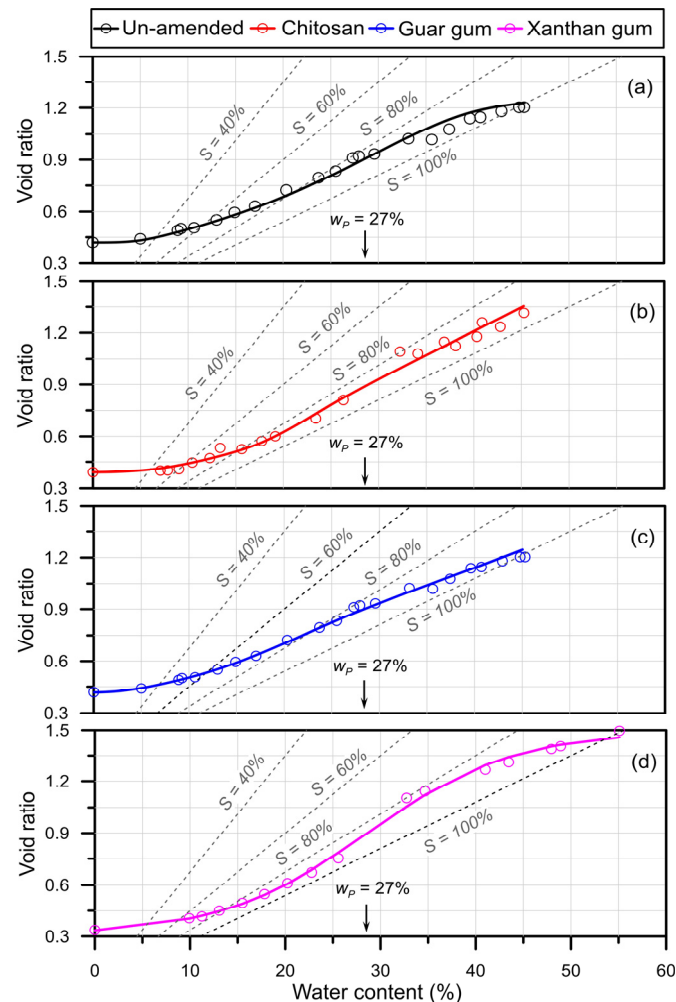


Figure 5. Swell–shrink curves for the optimally compacted expansive soil: (a) unamended and amended with (b) chitosan; (c) guar gum; (d) xanthan gum.

Table 4. Summary of shrinkage stages along the swell–shrink path.

Sample	Structural Stage		Normal Stage		Residual Stage	
	e Range	Δe	e Range	Δe	e Range	Δe
Unamended	1.23–1.11	0.12	1.11–0.60	0.51	0.60–0.43	0.17
Chitosan	—	—	1.31–0.52	0.63	0.52–0.39	0.13
Guar gum	—	—	1.20–0.50	0.55	0.50–0.42	0.08
Xanthan gum	1.50–1.32	0.18	1.32–0.49	0.83	0.49–0.34	0.15

The chitosan-amended soil (Figure 5b) and the guar-gum-amended soil (Figure 5c) showed a homogenous clay matrix with a uniform pore size distribution following *j*-shaped

paths exhibiting only normal (e from 1.31 to 0.52 and from 1.2 to 0.5, respectively) and residual shrinkage stages (e from 0.52 to 0.39 and from 0.5 to 0.42, respectively). The removal of structural shrinkage is attributed to healing of inter-aggregate pores and the development of a homogenous clay matrix. Clearly, these amended soils behave similar to those compacted on the wet side of optimum. The xanthan-gum-amended soil (Figure 5d) followed a distinct *s*-shaped path comprising all shrinkage stages (e from 1.5 to 1.32, 1.32 to 0.49, and 0.49 to 0.34, respectively) due to the partial healing of the larger pores. Moreover, the more pronounced *s*-path, when compared with the unamended soil, is attributed to the ability of this biopolymer to hold up to 2000% water mass with respect to its own mass [21,53]. For all the samples, most of the volume decrease occurred during normal shrinkage, which corresponded to a degree of saturation of $85 \pm 5\%$. Finally, the normal shrinkage for all the samples was bisected by the plastic limit (27%) of the unamended soil.

Figure 6 gives the swell–consolidation test results for the optimally compacted expansive clay. The unamended soil (Figure 6a) showed a vertical void ratio increase due to the particle swelling owing to water inundation, followed by a gradual void ratio decrease due to pore water expulsion under load and then by a low void ratio increase due to the rebound upon load removal. The C_c (0.313) and C_s (0.095) were similar to those in previous studies [40,54].

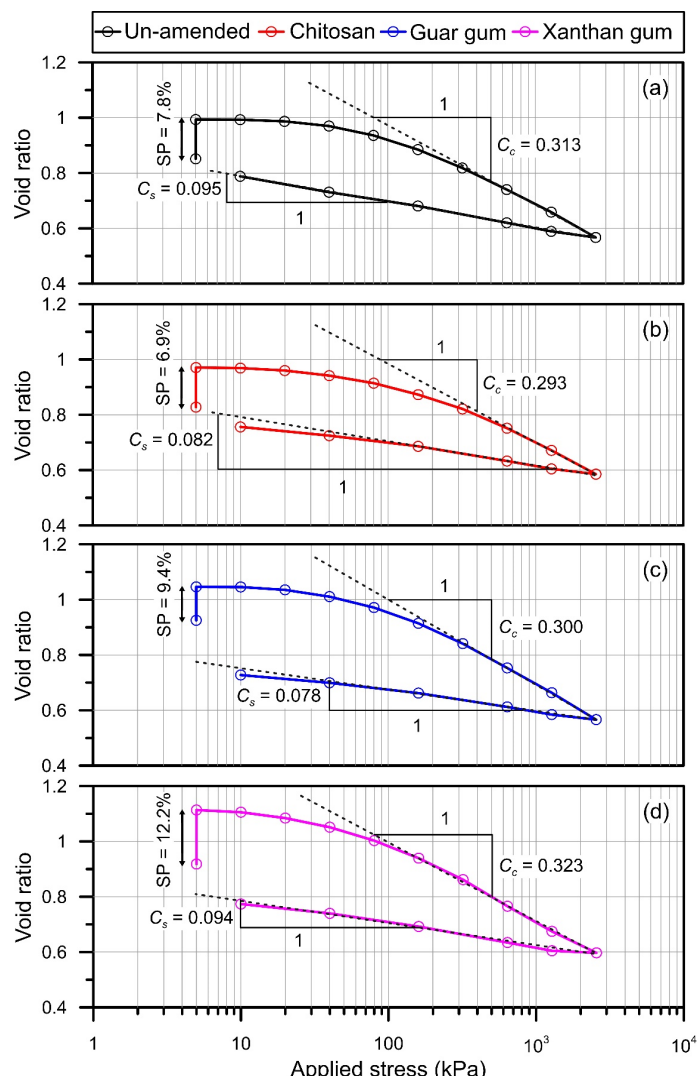


Figure 6. Swell–consolidation test results for the optimally compacted expansive soil: (a) un-amended and amended with (b) chitosan; (c) guar gum; (d) xanthan gum.

All of the biopolymer-amended samples followed the same trend as the unamended soil and showed closely matching values for C_c (0.31 ± 0.02) and C_s (0.08 ± 0.01). These ranges are similar to those observed by [29–31,55] and indicate that the effect of the biopolymer amendment on the consolidation parameters of the investigated expansive soil is negligible. This is because loading cancels the effect of the void ratio increase irrespective of the singular or dual porosity of the soil.

Figure 7 gives the swelling potential (SP) versus time at a 5 kPa seating stress for the investigated clay. The unamended soil exhibited a typical *s*-shaped swelling path comprising three swelling stages [56,57]: an *initial* relatively flat slope owing to water percolation through the originally unsaturated soil (2–8 h); (ii) a *primary* distinctly steep slope associated with an established wetting front (2–4 days); and (iii) a *secondary* fairly mild slope due to the near-saturation condition of the sample (2 weeks). The SP values for the unamended soil measured 7.8%.

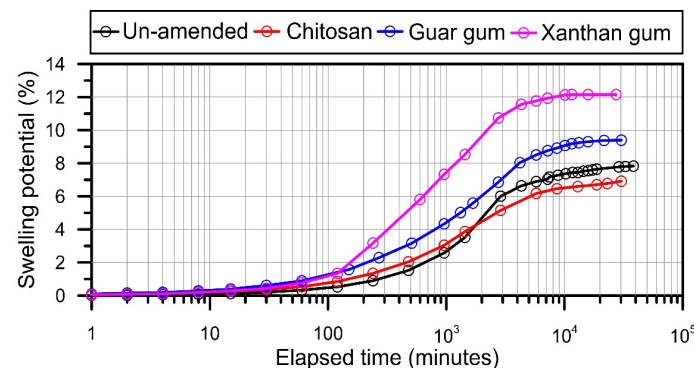


Figure 7. Swelling potential versus time under 5 kPa seating pressure.

All of the biopolymer-amended samples also showed *s*-shaped swelling potential paths. The SP values slightly decreased to 6.9% for the chitosan-amended soil and increased to 9.4% and 12.2% for the guar-gum-amended soil and xanthan-gum-amended soil, respectively. These results are in line with reported testing data such a swell pressure decrease from 53 kPa to 37 kPa due to a 0.12% chitosan addition and an increase to 58 kPa due to 1.5% guar gum amendment for a high-plasticity clay from Gujarat, India [33]. In contrast, an SP increase from 5% (using 0.5% xanthan gum) to 20% (using 2% xanthan gum) was observed for a similar high-plasticity clay from Indonesia [55]. These observations should be attributed to increased water adsorption because of the high hydrophilicity of the biopolymers and soil microstructural changes owing to variable biopolymer compositions with differences in charge type, charge density, and molecular weight [21,58]. The authors are currently investigating the detailed physicochemical interactions and fabric evolution for each biopolymer.

Figure 8 gives the change in saturated hydraulic conductivity (k_s) with respect to changes in the void ratio during consolidation under an applied stress ranging from 10 kPa to 2560 kPa. The combined data for all the samples (unamended soil and biopolymer-amended samples) were found to mostly fall within one standard deviation from the best fit ($R^2 = 0.8$). The k_s was found to decrease by three orders of magnitude (7×10^{-9} m/s to 1.6×10^{-12} m/s) over a void ratio decrease from 1.1 to 0.6. This decrease in k_s is similar to a reduction of more than two orders of magnitude from $\sim 10^{-9}$ m/s to $\sim 10^{-11}$ m/s, as reported by [55]. This general trend is attributed to a gradual pore size reduction during consolidation [59], with variations in the data associated with microstructural evolution due to the various biopolymers. The k_s data for the chitosan-amended soil and guar-gum-amended soil are lower than for the unamended sample. This is similar to the behavior of a soil compacted on the wet side of optimum. The relatively higher values in the void ratio for the xanthan-gum-amended soil are attributed to the high SP of this sample (Figure 7).

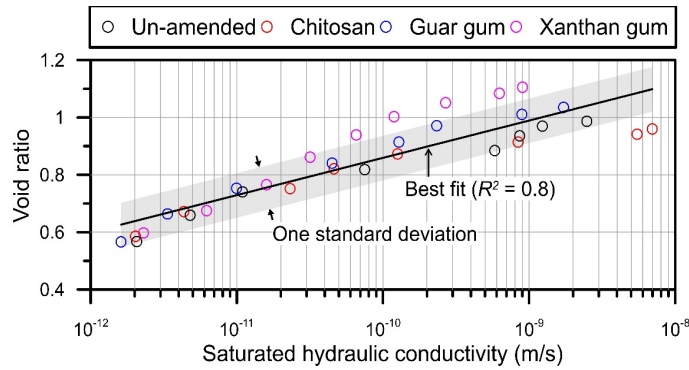


Figure 8. Variation in saturated hydraulic conductivity with void ratio during consolidation for the investigated expansive soil and the biopolymer-amended soils.

Figure 9 shows the variation in the consolidation parameters for the investigated expansive soil. The coefficient of consolidation (c_v) was calculated using the square root of time method expressed in the following equation [60]:

$$c_v = \frac{H_{dr}^2 T_{90}}{t_{90}} \quad (1)$$

where H_{dr} is one half of the average height of the specimen (double drainage); T_{90} is the time factor corresponding to a degree of consolidation of 90% (0.848); and t_{90} is the time corresponding to a 90% degree of consolidation. Likewise, the coefficient of the volume compressibility (m_v) was calculated from the slope of the compression curve under an instantaneous consolidation pressure [37]. Hanna et al. [61] extended the time rate of dissipation to a constant rate of loading to express the degree of consolidation using a time factor and found a 10% difference in the consolidation parameters obtained using the previous method.

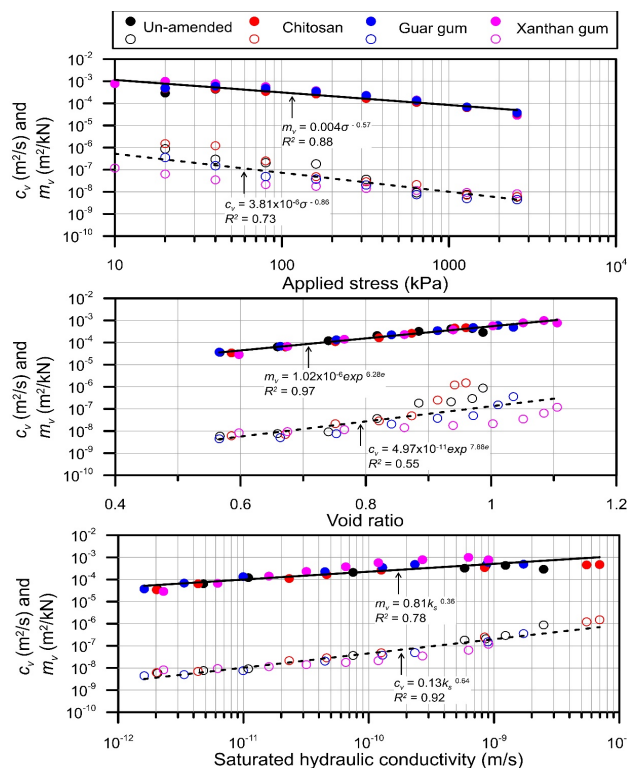


Figure 9. Variation in consolidation parameters for the investigated expansive soil and the biopolymer-amended soils.

As expected, both c_v and m_v in Figure 9 for the unamended soil and the biopolymer-amended samples decreased with applied stress and increased with the void ratio and hydraulic conductivity. Generally, the data fitted well (R^2 ranging from 0.97 to 0.55) with the trend lines such that the scatter cannot be attributed to variations in the biopolymers. The relatively low correlation coefficient ($R^2 = 0.55$) of the c_v-e relationship is attributed to the errors associated with the graphical determination of c_v . Muntohar [62] concluded for applied consolidation stresses higher than 5 kPa, the square root of time method gives accurate c_v values consistent with other common methods such as Feng and Lee [63], Robinson and Allam [64], and Mesri et al. [65].

4. Summary and Conclusions

The main contribution of this research was to understand the flow through and volume change behavior of compacted expansive soils amended with natural biopolymers. The efficacy of natural biopolymers for ameliorating the known geotechnical behavior of a regional expansive soil was investigated. The soil was amended using a 0.5% dosage of cationic chitosan, charge-neutral guar gum, and anionic xanthan gum during compaction. The flow through and volume change properties of the investigated expansive soil were affected as follows:

- The dual porosity (characterized by low air entry due to inter-aggregate pores and high air entry due to the clay matrix) of the soil was healed using chitosan and guar gum but was enhanced by xanthan gum.
- The *s*-shaped swell–shrink path (comprising structural, normal, and residual stages) of the soil was converted into a *j*-shaped path (no structural volume change) using chitosan and guar gum but was reverted back to a more pronounced form using xanthan gum.
- The consolidation behavior of the soil was largely unaffected by the addition of biopolymers such that the saturated hydraulic conductivity decreased from 10^{-9} m/s to 10^{-12} m/s under a void ratio decrease from 1.1 to 0.6.
- At a seating stress of 5 kPa, the swelling potential (7.8%) of the soil slightly decreased to 6.9% through the addition of chitosan but was found to increase to 9.4% and 12.2% for guar gum and xanthan gum, respectively.

The findings of this research indicate that the use of chitosan and guar gum will allow for the compaction of the investigated expansive soil on the dry side of optimum. This will reduce the susceptibility of the expansive clay to swelling and shrinkage by converting the soil from dual-porosity soil into uniform-porosity soil. The added benefit of using these biopolymers will be a decrease in hydraulic conductivity (albeit a minor increase in volume compressibility) and reduced water requirements during compaction on the dry side of optimum.

The observed flow through and volume change behavior of the investigated expansive clay in response to amendment is governed by biopolymer–clay–water interactions. The geotechnical understanding developed in this study provides a baseline and can be extended to other types of expansive clays with known engineering properties. Several factors affecting the physiochemical mechanisms and adsorption rates of biopolymers in active clay particle surfaces should be investigated. Specifically, micro-fabric visualization of particle associations such as bridging and patching can provide a fundamental-level understanding that can be applied more widely.

Author Contributions: Investigation, A.B.; data curation and analysis, A.B.; conceptualization, S.A.; supervision, S.A.; writing—original draft, A.B.; writing—review and editing, S.A. All authors have read and agreed to the published version of the manuscript.

Funding: This research was funded by the Natural Science and Engineering Research Council of Canada through a discovery grant to the corresponding author.

Data Availability Statement: The data presented in this study are openly available in article.

Acknowledgments: The authors thank the University of Regina for providing the laboratory space and computing facilities.

Conflicts of Interest: The authors declare there are no conflicts of interest.

References

1. Huang, J.; Kogbara, R.B.; Hariharan, N.; Masad, E.A.; Little, D.N. A State-of-the-Art Review of Polymers Used in Soil Stabilization. *Constr. Build. Mater.* **2021**, *305*, 124685. [[CrossRef](#)]
2. Agbovi, H.K. Biopolymer Flocculant Systems and Their Chemically Modified Forms for Aqueous Phosphate and Kaolinite Removal. Ph.D. Thesis, University of Saskatchewan, Saskatoon, SK, Canada, 2020.
3. Theng, B.K.G. *Formation and Properties of Clay-Polymer Complexes*, 2nd ed.; Elsevier Science: Amsterdam, The Netherlands, 2012; Volume 4.
4. Guo, M.Q.; Hu, X.; Wang, C.; Ai, L. Polysaccharides: Structure and Solubility. In *Solubility of Polysaccharides*; InTech: Bolton, UK, 2017. [[CrossRef](#)]
5. Armistead, S.J.; Smith, C.C.; Staniland, S.S. Sustainable Biopolymer Soil Stabilization in Saline Rich, Arid Conditions: A ‘Micro to Macro’ Approach. *Sci. Rep.* **2022**, *12*, 2880. [[CrossRef](#)]
6. Chang, I.; Lee, M.; Tran, A.T.P.; Lee, S.; Kwon, Y.M.; Im, J.; Cho, G.C. Review on Biopolymer-Based Soil Treatment (BPST) Technology in Geotechnical Engineering Practices. *Transp. Geotech.* **2020**, *24*, 100385. [[CrossRef](#)]
7. Lee, M.; Kwon, Y.M.; Park, D.Y.; Chang, I.; Cho, G.C. Durability and Strength Degradation of Xanthan Gum Based Biopolymer Treated Soil Subjected to Severe Weathering Cycles. *Sci. Rep.* **2022**, *12*, 19453. [[CrossRef](#)]
8. Chiellini, E.; Corti, A.; D’Antone, S.; Solaro, R. Biodegradation of Poly (Vinyl Alcohol) Based Materials. *Prog. Polym. Sci.* **2003**, *28*, 963–1014. [[CrossRef](#)]
9. Niaounakis, M. *Biopolymers: Applications and Trends*; Elsevier Inc.: Waltham, MA, USA, 2015; ISBN 9780323266987.
10. Lawrie, G.; Keen, I.; Drew, B.; Chandler-Temple, A.; Rintoul, L.; Fredericks, P.; Grøndahl, L. Interactions between Alginate and Chitosan Biopolymers Characterized Using FTIR and XPS. *Biomacromolecules* **2007**, *8*, 2533–2541. [[CrossRef](#)] [[PubMed](#)]
11. Abdou, E.S.; Nagy, K.S.A.; Elsabee, M.Z. Extraction and Characterization of Chitin and Chitosan from Local Sources. *Bioresour. Technol.* **2008**, *99*, 1359–1367. [[CrossRef](#)]
12. Mudgil, D.; Barak, S.; Khatkar, B.S. Guar Gum: Processing, Properties and Food Applications—A Review. *J. Food Sci. Technol.* **2014**, *51*, 409–418. [[CrossRef](#)]
13. Muguda-Viswanath, S. Biopolymer Stabilized Earthen Construction Materials. Ph.D. Thesis, Durham University, Durham, UK, 2019.
14. Soldo, A.; Miletic, M.; Auad, M.L. Biopolymers as a Sustainable Solution for the Enhancement of Soil Mechanical Properties. *Sci. Rep.* **2020**, *10*, 267. [[CrossRef](#)] [[PubMed](#)]
15. Chang, I.; Im, J.; Prasidhi, A.K.; Cho, G.C. Effects of Xanthan Gum Biopolymer on Soil Strengthening. *Constr. Build. Mater.* **2015**, *74*, 65–72. [[CrossRef](#)]
16. Latifi, N.; Vahedifard, F.; Ghazanfari, E.; Horpibulsuk, S.; Marto, A.; Williams, J. Sustainable Improvement of Clays Using Low-Carbon Nontraditional Additive. *Int. J. Geomech.* **2018**, *18*, 04017162. [[CrossRef](#)]
17. Deng, Y.; Dixon, J.B.; White, G.N. Bonding Mechanisms and Conformation of Poly(Ethylene Oxide)-Based Surfactants in Interlayer of Smectite. *Colloid. Polym. Sci.* **2006**, *284*, 347–356. [[CrossRef](#)]
18. Labille, J.; Thomas, F.; Milas, M.; Vanhaeverbeke, C. Flocculation of Colloidal Clay by Bacterial Polysaccharides: Effect of Macromolecule Charge and Structure. *J. Colloid. Interface Sci.* **2005**, *284*, 149–156. [[CrossRef](#)]
19. Bhalkaran, S.; Wilson, L. Investigation of Self-Assembly Processes for Chitosan-Based Coagulant-Flocculant Systems: A Mini-Review. *Int. J. Mol. Sci.* **2016**, *17*, 1662. [[CrossRef](#)]
20. Mahmood, A.; Patel, D.; Hickson, B.; Desrochers, J.; Hu, X. Recent Progress in Biopolymer-Based Hydrogel Materials for Biomedical Applications. *Int. J. Mol. Sci.* **2022**, *23*, 1415. [[CrossRef](#)]
21. Zhou, C.; So, P.S.; Chen, X.W. A Water Retention Model Considering Biopolymer-Soil Interactions. *J. Hydrol.* **2020**, *586*, 124874. [[CrossRef](#)]
22. Gu, B.; Doner, H. *The Interaction of Polysaccharides with Silver Hill Illite*; Springer: Berlin/Heidelberg, Germany, 1992; Volume 40.
23. Razali, M.A.A.; Ahmad, Z.; Ahmad, M.S.B.; Ariffin, A. Treatment of Pulp and Paper Mill Wastewater with Various Molecular Weight of PolyDADMAC Induced Flocculation. *Chem. Eng. J.* **2011**, *166*, 529–535. [[CrossRef](#)]
24. Manzanal, D.; Orlandi, S.; Fernandez, M.; Laskowski, C.; Barría, J.C.; Codevila, M.; Piqué, T. Soil Water Retention of Highly Expansive Clay Stabilized with a Biopolymer. *MATEC Web Conf.* **2021**, *337*, 01006. [[CrossRef](#)]
25. Rahmati, M.; Pohlmeier, A.; Abasiyan, S.M.A.; Weihermüller, L.; Vereecken, H. Water Retention and Pore Size Distribution of a Biopolymeric-Amended Loam Soil. *Vadose Zone J.* **2019**, *18*, 1–13. [[CrossRef](#)]
26. Tran, T.P.A.; Cho, G.-C.; Ilhan, C. Water Retention Characteristics of Biopolymer Hydrogel Containing Sandy Soils. *Hue Univ. J. Sci. Earth Sci. Environ.* **2020**, *129*, 4A. [[CrossRef](#)]
27. Lukjan, A.; Iyaruk, A.; Petchprakob, C. Soil Water Retention Curve and Permeability Function of the Para Rubber Biopolymer Treated Sand. *Interdiscip. Res. Rev.* **2020**, *15*, 1–7.

28. Wong, J.T.F.; Chen, Z.; Wong, A.Y.Y.; Ng, C.W.W.; Wong, M.H. Effects Of Biochar on Hydraulic Conductivity of Compacted Kaolin Clay. *Environ. Pollut.* **2018**, *234*, 468–472. [CrossRef] [PubMed]
29. Vydehi, K.V.; Moghal, A.A.B. Effect of Biopolymeric Stabilization on the Strength and Compressibility Characteristics of Cohesive Soil. *J. Mater. Civ. Eng.* **2022**, *34*, 04021428. [CrossRef]
30. Ni, J.; Li, S.S.; Geng, X.Y. Mechanical And Biodeterioration Behaviours of a Clayey Soil Strengthened with Combined Carrageenan and Casein. *Acta Geotech.* **2022**, *17*, 5411–5427. [CrossRef]
31. Vydehi, K.V.; Moghal, A.A.B. Compressibility Characteristics of Guar Gum-Treated Expansive Soil. In *Indian Geotechnical Conference: Ground Improvement and Reinforced Soil Structures*; Reddy, S., Saride, S., Krishna, M., Eds.; Springer: Berlin/Heidelberg, Germany, 2022; pp. 339–345.
32. Holtz, R.D.; Kovacs, W.D.; Sheahan, T.C. *An Introduction to Geotechnical Engineering*; Pearson: Upper Saddle River, NJ, USA, 2011; ISBN 9780130317216.
33. Parmar, J.; Yadav, V.; Pandya, S. Influence of Biopolymer Treatment on Suction Characteristics of Bhavnagar Expansive Soil. In *Lecture Notes in Civil Engineering*; Springer Science and Business Media Deutschland GmbH: Berlin/Heidelberg, Germany, 2022; Volume 152, pp. 471–487.
34. Chang, I.; Im, J.; Cho, G.C. Introduction Of Microbial Biopolymers in Soil Treatment for Future Environmentally-Friendly and Sustainable Geotechnical Engineering. *Sustainability* **2016**, *8*, 251. [CrossRef]
35. Puppala, A.; Pedarla, A. Innovative Ground Improvement Techniques for Expansive Soils. *Innov. Infrastruct. Solut.* **2017**, *2*, 24. [CrossRef]
36. Prakash, K.; Sridharan, A.; Ananth Baba, J.; Thejas, H.K. Determination of Shrinkage Limit of Fine-Grained Soils by Wax Method. *Geotech. Test. J.* **2009**, *32*, 86–89. [CrossRef]
37. Terzaghi, K.; Peck, R.B.; Mesri, G. *Soil Mechanics in Engineering Practice*, 3rd ed.; John Wiley & Sons Inc.: New York, NY, USA, 1996.
38. Azam, S.; Ito, M.; Chowdhury, R. Engineering Properties of an Expansive Soil. In Proceedings of the 18th International Conference on Soil Mechanics and Geotechnical Engineering, Paris, France, 2–6 September 2013; pp. 199–202.
39. Ito, M.; Azam, S. Engineering Properties of a Vertisolic Expansive Soil Deposit. *Eng. Geol.* **2013**, *152*, 10–16. [CrossRef]
40. Azam, S.; Chowdhury, R.H. Swell-Shrink-Consolidation Behavior of Compacted Expansive Clays. *Int. J. Geotech. Eng.* **2013**, *7*, 424–430. [CrossRef]
41. Ito, M.; Azam, S. Swell-Shrink-Consolidation Behaviour of Expansive Regina Clay. In Proceedings of the GeoHalifax, Halifax, NS, Canada, 20–24 September 2009; pp. 829–834.
42. Wong, C.; Wan, R.; Wong, R. Some Observations in Soil-Pipe Model Tests under Vertical Uplift Loading in Compacted Clay. *Int. J. Phys. Model. Geotech.* **2022**, *22*, 113–127. [CrossRef]
43. Chowdhury, R.H.; Azam, S. Unsaturated Shear Strength Properties of a Compacted Expansive Soil from Regina, Canada. *Innov. Infrastruct. Solut.* **2016**, *1*, 47. [CrossRef]
44. Paranthaman, R.; Azam, S. Effect of Compaction on Desiccation and Consolidation Behavior of Clay Tills. *Innov. Infrastruct. Solut.* **2022**, *7*, 31. [CrossRef]
45. Leroueil, S.; Hight, D.W. Compacted Soils: From Physics to Hydraulic and Mechanical Behaviour. In *Advances in Unsaturated Soils*; CRC Press: Boca Raton, FL, USA, 2013; ISBN 9780203771075.
46. Ito, M.; Azam, S.; Clifton, W. Suction-Based Model for Predicting Cyclic and Transient Volume Changes in Expansive Clays Using a Material Property Function. *Eng. Geol.* **2022**, *296*, 106491. [CrossRef]
47. Burton, G.J.; Pineda, J.A.; Sheng, D.; Airey, D. Microstructural Changes of An Undisturbed, Reconstituted and Compacted High Plasticity Clay Subjected to Wetting and Drying. *Eng. Geol.* **2015**, *193*, 363–373. [CrossRef]
48. Khalid, N.; Mukri, M.; Kamarudin, F.; Abdul Ghani, A.H. Effect of Compaction Characteristics on Hydraulic Conductivity Performance for Sedimentary Residual Soil Mixed Bentonite as Compacted Liners. In Proceedings of the IOP Conference Series: Earth and Environmental Science, Florence, Italy, 4–27 September 2019; Institute of Physics Publishing: Bristol, UK, 2020; Volume 498.
49. Das, B.M.; Sobhan, K. *Principles of Geotechnical Engineering*, 9th ed.; Cengage Learning: Boston, MA, USA, 2018.
50. Zhang, Y.; Yang, Z.; Wang, F.; Zhang, X. Comparison of Soil Tortuosity Calculated by Different Methods. *Geoderma* **2021**, *402*, 115358. [CrossRef]
51. Bukhary, A.; Azam, S. A Review of Physicochemical Stabilization for Improved Engineering Properties of Clays. *Geotechnics* **2023**, *3*, 744–759. [CrossRef]
52. Umezakin, T.; Kawamura, T. Shrinkage and Desaturation Properties during Desiccation of Reconstituted Cohesive Soil. *Soils Found.* **2013**, *53*, 47–63. [CrossRef]
53. Tran, T.P.A.; Im, J.; Cho, G.-C.; Chang, I. Soil-Water Characteristics of Xanthan Gum Biopolymer Containing Soils. In Proceedings of the 19th International Conference on Soil Mechanics and Geotechnical Engineering, Seoul, Republic of Korea, 17–21 September 2017; pp. 1091–1094.
54. Ito, M.; Azam, S. Engineering Characteristics of a Glacio-Lacustrine Clay Deposit in a Semi-Arid Climate. *Bull. Eng. Environ.* **2009**, *68*, 551–557. [CrossRef]
55. Kwon, Y.M.; Chang, I.; Cho, G.C. Consolidation and Swelling Behavior of Kaolinite Clay Containing Xanthan Gum Biopolymer. *Acta Geotech.* **2023**, *18*, 3555–3571. [CrossRef]

56. Mishra, A.K.; Dhawan, S.; Rao, S.M. Analysis of Swelling and Shrinkage Behavior of Compacted Clays. *Geotech. Geol. Eng.* **2008**, *26*, 289–298. [[CrossRef](#)]
57. Ito, M.; Azam, S. Relation between Flow through and Volumetric Changes in Natural Expansive Soils. *Eng. Geol.* **2020**, *279*, 105885. [[CrossRef](#)]
58. Jung, J.; Ku, T.; Ahn, J. Small Strain Stiffness of Unsaturated Sands Containing a Polyacrylamide Solution. *Materials* **2017**, *10*, 401. [[CrossRef](#)]
59. Romero, E.; Della Vecchia, G.; Jommi, C. An Insight into the Water Retention Properties of Compacted Clayey Soils. *Geotechnique* **2011**, *61*, 313–328. [[CrossRef](#)]
60. Taylor, D. *Fundamentals of Soil Mechanics*; J. Wiley and Sons: New York, NY, USA, 1948.
61. Hanna, D.; Sivakugan, N.; Lovisa, J. Simple Approach to Consolidation Due to Constant Rate Loading in Clays. *Int. J. Geomech.* **2013**, *13*, 193–196. [[CrossRef](#)]
62. Muntohar, A. Reliability of the Method for Determination of Coefficient of Consolidation (C_v). In Proceedings of the 13th Annual Scientific Meeting, Denpasar, Bali, 5 November 2009; pp. 70–74.
63. Feng, T.-W.; Lee, Y.-J. Coefficient of Consolidation from the Linear Segment of the $T_1/2$ Curve. *Can. Geotech. J.* **2001**, *38*, 901–909. [[CrossRef](#)]
64. Robinson, R.; Allam, M. Determination of Coefficient of Consolidation from Early Stage of Log t Plot. *Geotech. Test. J.* **1996**, *19*, 316. [[CrossRef](#)]
65. Mesri, G.; Feng, T.W.; Shahien, M. Coefficient of Consolidation by Inflection Point Method. *J. Geotech. Geoenviron. Eng.* **1999**, *125*, 716–718. [[CrossRef](#)]

Disclaimer/Publisher's Note: The statements, opinions and data contained in all publications are solely those of the individual author(s) and contributor(s) and not of MDPI and/or the editor(s). MDPI and/or the editor(s) disclaim responsibility for any injury to people or property resulting from any ideas, methods, instructions or products referred to in the content.